Biosensors and Bioelectronics xx (xxxx) xxxx–xxxx

Contents lists available at ScienceDirect

Biosensors and Bioelectronics

journal homepage: www.elsevier.com/locate/bios

Multienzyme decorated polysaccharide amplified electrogenerated chemiluminescence biosensor for cytosensing and cell surface carbohydrate profiling

Ling Zhang[1], Yangzhong Wang[1], Qianqian Tian, Yang Liu, Jinghong Li*

Department of Chemistry, Key Laboratory of Bioorganic Phosphorus Chemistry & Chemical Biology, Beijing Key Laboratory for Microanalytical Methods and Instrumentation, Tsinghua University, Beijing 100084, China

ARTICLE INFO

Keywords:
Multienzyme decorated polysaccharide
Signal amplification
Carbohydrate
Cytosensing
ECL
Con A

ABSTRACT

A novel ECL biosensor for cytosensing and cell surface carbohydrate expression evaluation was developed, by the integration of the peptide modified interface for highly specific carbohydrate recognition and sodium alginate loaded glucose oxidase as the signal probe with high signal amplification efficiency. A cysteine-terminated peptide self-assembled on the electrode through Au–S bond to construct a functional interface for cell capture, with decent biocompatibility and high affinity for the human breast cancer cell MCF-7. Concanavalin A lectin modified gold nanoparticles specifically recognized the cell surface carbohydrates and were absorbed on the electrode, followed by the immobilization of multiple glucose oxidase conjugated sodium alginate, which could remarkably increase the sensitivity of the biosensor with enhanced catalysis. The as-proposed ECL cytosensor was successfully applied for the detection of the MCF-7 tumor cells, whose glycans on the cell membranes are over-expressed. A low detection limit of 150 cells mL^{-1} was obtained, with a wide dynamic linear range from 5.0×10^{2} to 5.0×10^{5} cells mL^{-1}. Due to the excellent sensitivity, stability and biocompatibility, the ECL biosensor would be promising in reliable diagnostics of glycan relevant biomarkers for cancer and other diseases.

1. Introduction

Cells are covered by a number of glycans which are covalently bound to the underlying proteins or lipids with high density and complex diversity (Linhardt and Toshihiko, 2004). The carbohydrates on the cell membrane possess abundant information for specific molecular recognition and play important roles for cell migration, proliferation and communication (Dennis et al., 2009; Hirabayashi, 2008). Its abnormal expression has been proved to be related with many diseases, especially Alzheimer's disease and cancers (Rexach et al., 2008; Zhao et al., 2008). Therefore, developing glyco-biosensors for synchronously cytosensing and cell surface carbohydrate expression analysis is significant in clinical diagnostics. It will provide a platform to understand the roles of carbohydrates in disease progression and monitor the glycan relevant biomarkers. Recently, a serious of approaches have been developed for probing carbohydrate-protein interactions, cell surface carbohydrates profiling and cytosensing, including electrochemical impedance spectroscopy (Hu et al., 2013), quartz crystal microbalance (Shen et al., 2007), fluorescence polarization (Kakehi et al., 2001), localized surface plasmon resonance (Bellapadrona et al., 2012), and field effect transistors (Vedala et al., 2011). However, the sensitivity and stability in most of these methods are still limited, because the modifications on the biosensing interfaces induce the less active accessibility and weak affinity between monosaccharides and lectin as well as the loss of biocompatibility. Fluorescent assays also have drawbacks such as false positives, high background and complicated labelling procedures. Thus, it is still a critical demand on simple, rapid, and low-cost detection technologies for the accurate and sensitive analysis of cancer cells and profiling of cell surface carbohydrates.

To avoid the loss of biocompatibility and weak recognition affinity, some peptides have been used for targeting different tumors and cell types (Zhang et al., 2001; Stangl et al., 2014). Among these, tumor homing peptides RGD could target the $\alpha_v\beta3$ integrin in the tumor cells and NGR could recognize aminopeptidase N receptors in the vasculature (Zitzmann et al., 2002; Corti et al., 2008). Besides, peptides arrays formed by short peptides covalently bound to a solid surface showed specific binding affinity to the cells (Veiseh et al., 2007).

* Corresponding author.
E-mail address: jhli@mail.tsinghua.edu.cn (J. Li).
[1] These two authors contributed equally to this study and share first authorship.

http://dx.doi.org/10.1016/j.bios.2016.10.040
Received 19 August 2016; Received in revised form 2 October 2016; Accepted 18 October 2016
Available online xxxx
0956-5663/

Combining with their high specificity, strong binding force and biocompatibility, peptides show brilliant prospect for developing sensing interface for the cancer cells.

Electrogenerated chemiluminescence (ECL) technique, which involves electron-transfer reactions and light-emitting process of the luminophores on the electrode (Richter, 2004; Marquette and Blum, 2009), is a powerful analytical tool with advantages of low cost, low background noise, wide dynamic concentration response range and high sensitivity (Liu et al., 2015). It has been widely applied in small molecule detection (Wang et al., 2009), immunoassay (Xu et al., 2011), cell analysis (Han et al., 2011) and clinical diagnosis (Zhang et al., 2012). Meanwhile, on account of the good biocompatibility, fascinating electrocatalytic activity, large surface area, and excellent conductivity, nanomaterials such as gold nanoparticles (Li et al., 2016), quantum dots (Li and Zhu, 2013), metal oxide nanorods (Lu et al., 2006), carbon nanotubes (Zhang et al., 2004) and graphene (Zhang et al., 2014) have been widely used in electrochemistry, biosensing and imaging. The unique properties of nanomaterials allow them to be interfaced with biomolecules and open up a wide range of biological applications (Cha et al., 2013; Wang et al., 2014a, 2014b; Guo et al., 2014). Nanomaterials can also function as efficient carriers for multiple carbohydrate presentation to achieve sufficiently high affinities required for sensitive recognition and labels for signal amplification. (Wang et al., 2003; Zhang et al., 2007).

In this work, a sensitive ECL biosensor, using peptides as capture probes, Concanavalin A (Con A) modified gold nanoparticles (Con A@AuNPs) as multiple-site combined probes and glucose oxidase conjugated sodium alginate (GOx@SA) as nanoprobes, was developed for selectively cancer cell detection and cell surface carbohydrate expression evaluation (Scheme 1). To demonstrate the principle, a specific peptide for human breast cancer cell MCF-7 cell was chosen as capture probe. Glucose oxidase, an important mannose-containing glycoprotein (Wilson and Turner, 1992), was used to catalyze the oxidation of glucose to produce hydrogen peroxide which significantly improves the ECL signal of luminol (Wang et al., 2013). Con A, which has specific affinities to the sodium alginate, the mannose on GOx, and glycan on the cell surface, served as the recognizer for cell surface carbohydrates and the capturer for GOx@SA nanoprobes. Sodium alginate, a kind of natural polysaccharide composed by L-mannuronic acid and D-guluronic acid at a certain proportion, which could interact with Concanavalin A (Con A) (Holme et al., 2008), was used as the carrier to load multiple GOx with plenty of carboxylic acid on its structure, to form the signal probe. Owing to its good hydrophily, low adhesion and excellent biocompatibility, sodium alginate could fix the enzymes without damaging their structure and bioactivity (Prang et al., 2006). Moreover, sodium alginate provides much more recognition sites for the conjugation of biomolecules and dramatically improves the sensitivity and selectivity of the biosensor. The experimental observations indicate that this strategy can not only recognize the cells with high specificity but also detect the cell and its surface glycan with high sensitivity. Such a simple and sensitive biosensor would be promising in reliable diagnostics of glycan relevant biomarkers for cancer and other diseases.

2. Experimental section

2.1. Materials and reagents

Sodium Alginate (SA) and Coomassie Brilliant Blue G250 (G250) were provided by Aladdin (China). Bovine serum albumin (BSA) was purchased from Dingguo Biological Products Company (China). Glucose oxidase (GOx, 100–250 units per mg) was obtained from Sangon Biotech (China). Concanavalin A (Con A) and luminol were received from Sigma-Aldrich (USA). $HAuCl_4{\cdot}3H_2O$ (48% w/w) was obtained from Shanghai Regent (China). 1-(3-Dimethylaminopropyl)-3-ethylcarbodiimide hydrochloride (EDC) and N-Hydroxysuccinimide (NHS) were provided by Alfa Aesar (USA). Cysteine-terminated peptide WC10 (WLEAAYQRFLC, 98%) was purchased from GL Biochem (China). Other reagents of analytical grade were obtained from Sinopharm Chemical Reagent Company (China) and were used as received. 100 mM Phosphate buffer solutions (PBS) were prepared with $Na_2HPO_4{\cdot}12H_2O$ and $NaH_2PO_4{\cdot}2H_2O$, containing 137 mM NaCl

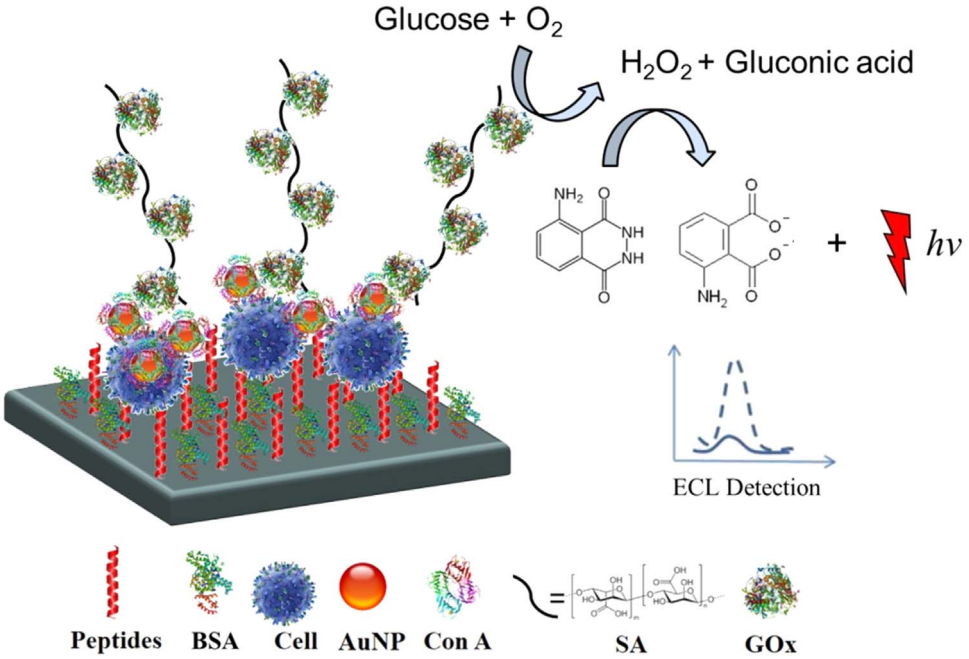

Scheme 1. Configuration of ECL biosensor for selective detection of cancer cell and cell surface carbohydrate profiling. The cysteine-terminated peptide is firstly immobilized on the gold electrode through the Au-S bond for specific recognition of cancer cell MCF-7. After cell capturing, BSA is used to block the electrode to avoid nonspecific adsorption. Then, the Con A lectin conjugated gold nanoparticles (Con A@Au NPs) are absorbed on the cell surface due to the affinity between Con A and glycans. Thereafter, the GOx modified sodium alginate (GOx@SA) is immobilized via the affinities between the oligosaccharides on sodium alginate/GOx and Con A lectins on Au NPs, which catalyzes the oxidation of glucose to produce hydrogen peroxide and significantly improve the ECL signal of luminol.

and 2.7 mM KCl.

2.2. Apparatus

The UV–Vis experiment was performed with a UV-3900 spectrophotometer (Hitachi, Japan). The Cyclic Voltammetry (CV) was conducted on a CHI 660b instrument (CH Instrument Co.). Electrochemical Impedance Spectroscopy (EIS) was carried out on a PARSTAT 2273 potentiostat/galvanostat (Advanced Measurement Technology Inc.) by applying an AC voltage of 10 mV amplitude in the 0.01 Hz to 10^5 Hz frequency range in a solution containing 5 mM $K_3[Fe(CN)_6]/K_4[Fe(CN)_6]$ and 0.1 M KCl. The ECL measurements were carried out on an MPI-B multifunctional electrochemical analytical system (Xi'an Remex Analytical Instrument Co., Ltd., China). If no special statement was made, the ECL measurements were performed in a 0.1 M PBS (pH 9.0) containing 100 μm luminol and 0.1 M glucose at a scan rate of 100 mV s^{-1} and the voltage of PMT was maintained at 600 V. Ag/AgCl electrode and platinum wire were used as the reference electrode and counter electrode, respectively.

2.3. Cell line, culture and treatment

The MCF-7, K562, HL60, Ramos cell lines were kindly provided by the medical college of Tsinghua University. MCF-7 cells were cultured in DMEM medium (Dingguo, China) supplemented with 10% fetal calf serum (Tianhang, China), 100 U mL^{-1} penicillin and 100 U mL^{-1} streptomycin at 37 ℃ in a humidified atmosphere of 5% CO_2. The cells in exponential growth phase were collected using trypsin (Dingguo, China) and separated by centrifugation at 800 rpm for 5 min. Then the cells were washed with sterile PBS (0.01 M, pH 7.4) twice. For K562, HL60 and Ramos cell lines, DMEM medium was replaced with RPMI 1640 medium, and the cells in exponential growth phase were collected and separated by centrifugation directly. The cell number was determined using a blood counting chamber.

2.4. Preparation of Con A conjugated gold nanoparticles and GOx conjugated SA

The gold nanoparticles were prepared as reported previously (Wang et al., 2014a, 2014b). In brief, 2.5 mL of 4 g mL^{-1} $HAuCl_4$ solution and 97.5 mL deionized water were added into a round flask and heated to boiling. Then, 5 mL of 10 mg mL^{-1} sodium citrate solution was added rapidly under vigorous stirring. The solution was maintained at the boiling state for 15 min until the colour changed from yellow to deep wine red, and the gold nanoparticles (AuNPs) formed. The Con A conjugated gold nanoparticles (Con A@AuNPs) were prepared by adding 120 μL Con A (5 mg mL^{-1}) to a 11 mL H_2O-diluted AuNPs solution (8:3). After being adjusted to pH 9.0, the mixture was gentle stirred for 4 h and centrifuged at 10,000 rpm for 10 min. Then the sediment was washed with deionized water and resuspended in 750 μL sterile PBS.

Alginates having glucose oxidase in the side were synthesized through standard carbodiimide chemistry. 20 mg sodium alginate was added to 2 mL morpholinoethanesulfonic acid (MES) buffer (0.1 M, pH 6.0) and stirred to get a homogeneous solution. Then the alginate was mixed with 2 mL EDC/NHS (100 mM/300 mM) for the activation of carbonyl groups in MES buffer for 10 min, followed by addition of 500 μL GOx solution (5 mg mL^{-1}) and gently stirred for 4 h. After being precipitated with ethanol, the mixture was centrifuged at 10,000 rpm for 10 min and washed with deionized water quickly. Finally, the sediment was re-suspended in 2 mL sterile PBS. The modification extent of an alginate by GOx was evaluated with Coomassie brilliant blue G250 staining and an UV–Vis spectrometer. The extent of alginate modification was calculated from the calibration curve obtained by measuring the absorbance at 595 nm of different percentages of GOx in G250 solution.

2.5. Biosensor fabrication

A gold electrode (GE, diameter of 2 mm) was polished carefully first with 0.3 μm α-Al_2O_3 slurry on an abrasive cloth and thoroughly cleaned with ethanol and deionized water under ultrasonication. Prior to immobilization of Con A, the gold electrode was scanned in 0.5 M H_2SO_4 between 0.2 and 1.65 V (vs. Ag/AgCl) until a reproducible cyclic voltammogram curve was obtained. After drying with N_2, the gold electrode was immersed in a 100 μL 65% acetonitrile/water solution containing 300 μm WC10 peptide for 6 h. The resulting electrode was soaked in ethanol for 30 s, followed by its incubation in sterile PBS for 30 min. Then the cell capture was performed by immersing the peptide modified electrode in 100 μL cell suspension at certain concentrations for 1 h at 37 °C. The incubation was done in PBS solution (pH 7.4), which is serum-free, in order to prevent the proteolytic effect of serum on the peptides. After being rinsed with PBS, the electrode was immersed in 1 mg mL^{-1} BSA for 1 h to block the nonspecific binding sites. The electrode was then carefully rinsed with PBS to remove the excess BSA. Subsequently, the electrode was immersed in a mixture containing 50 μL Con A@AuNPs, 10 μL 10 mM $CaCl_2$ and 10 μL 10 mM $MnCl_2$ for 30 min. Finally, the electrode was dipped in a mixture containing 40 μL GOx@SA, 10 μL sterile PBS, 10 μL 10 mM $CaCl_2$ and 10 μL 10 mM $MnCl_2$ for 1 h. All these incubations were performed at 37 °C. Then the electrode was washed with PBS and subjected to the ECL characterization.

3. Results and discussion

3.1. Multivalent recognition and highly selective cancer cells detection strategy

Scheme 1 displays the configuration of biosensor for selective detection of cancer cell. In this work, cysteine-terminated WC10 peptide is utilized to construct a functional interface through the Au-S bond, which has biocompatibility and high affinity for the P160 receptor of human breast cancer cell MCF-7 (Ahmed et al., 2010). After cell capturing, the electrode is blocked by BSA to avoid nonspecific adsorption. Due to the large surface area, Con A decorated gold nanoparticles are fabricated as the recognition probes. The Con A lectin can interact with glycan on cell surface, sodium alginate and glycan of the glycoprotein GOx. Furthermore, as Con A is a homotetramer and an individual gold nanoparticle is decorated by several Con A lectins, "multivalent effect" can be used to improve their affinities, which brings the biosensor with excellent stability. Finally, GOx modified alginate is used as a multifunctional signal probe, which can be gotten by covalently modifying glycoproteins on the carboxyl groups of sodium alginate. GOx is a glycoprotein, which is covered with oligosaccharide chains. Mannose in the form of oligosaccharide presented on the GOx surface can be specifically recognized by Con A. Besides, GOx also catalyzes the oxidation of glucose to produce hydrogen peroxide which significantly improves the ECL signal of luminol. In the presence of MCF-7 cells, the ECL signal of biosensor increases, which could be applied in selective detection of cancer cell.

3.2. Con A-decorated gold nanoparticles and gox-modified sodium alginates

The as-prepared Con A conjugated gold nanoparticles were characterized by UV–Vis. As shown in Fig. 1A, the characteristic absorption peak of gold nanoparticles red shifted from 520 nm to 525 nm after the decoration of Con A on gold nanoparticles (curve a and b). Additionally, Coomassie Brilliant Blue G250 was used to verify the successful modification of proteins on gold nanoparticles and alginate. The dye molecules bound to proteins to form a complex, which made the colour change from brownish to blue (Fig. 1C). Fig. 1A shows the UV–Vis absorption spectrum of Coomassie Brilliant Blue G250, which

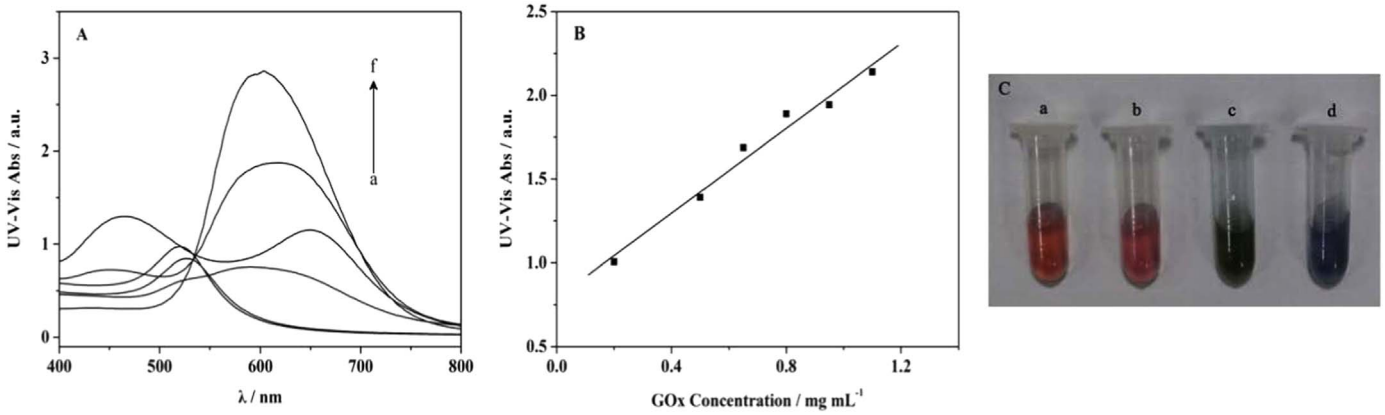

Fig. 1. (A) UV–Vis spectras of AuNPs (a), Con A@AuNPs (b), Con A@AuNPs adding G250 (c), G250 (d), GOx@SA adding G250 (e) and GOx adding G250 (f). (B) The linear relationship between the UV–Vis absorption intensity and the GOx concentration. (C) Photos of AuNPs (a), Con A@AuNPs (b), G250 (c), Con A@AuNPs adding G250 (d).

had the maximum wavelength at 465 nm and 650 nm (curve d). After adding the Con A@AuNPs or GOx@SA solution, the characteristic peak shifted to 595 nm (curve e and f) for the formation of protein-dye complex, which confirmed the successful conjugations of Con A on gold nanoparticles and GOx on alginate. The extent of alginate modification could be calculated from the calibration curve obtained by measuring the absorbance of different percentages of GOx in Coomassie Brilliant Blue G250 (Fig. 1B). The UV–Vis absorption intensities increased linearly with the GOx concentration over the range from 0.2 to 1.1 mg mL^{-1}. The linear regression equation is A=0.79+1.27×C with the correlation coefficient of R^2=0.99 (n=6), where A is the UV–Vis absorption intensities and C is the GOx concentration. From the absorption intensity of curve e in Fig. 1A, the GOx concentration could be calculated to be 5.4×10^{-6} M. Taking into account of the precipitation efficiency of alginate, which could be gotten from the weights of alginate before and after precipitated by ethanol, the amount of GOx on a alginate molecule was calculated to be 14. As GOx was a functional glycoprotein acting as a multivalent recognition unit and a signal amplification probe, the GOx modified alginate would greatly improve the sensitivity and stability of biosensor.

3.3. Electrochemical characterizations of the biosensor

The cyclic voltammetry (CV) was employed to evaluate the assembly processes by monitoring the electron transfer ability tunneling through the barrier layer between the electroactive probes and the gold electrode. Fig. 2A shows the CV curves presenting the step-by-step build up processes on the gold electrode using $Fe(CN)_6^{4-/3-}$ as electroactive probe. As can be seen, a couple of quasi-reversible redox peaks were obtained for gold electrode (curve a). When the electrode was treated with WC10, the cysteine-terminated peptides were immobilized on the gold electrode surface through the Au-S bond to form a dense assemble layer, which led to a decrease of peak current (curve b) for the electronically inert feature of peptides that partially blocked the electron transfer and mass transfer of $Fe(CN)_6^{4-/3-}$ couple ions at the electrode interface. After the capture of MCF-7 cells, the peak current in the CV decreased further and the potential gap between the anodic and cathodic peaks became wider (curve c) for that the cells were totally electronically inert. When BSA was added as the blocking layer, the peak current also decreased (curve d). Finally, Con A-modified gold nanoparticles and GOx-modified alginate were utilized as the signal probes, it was found that the peak current decreased further (curve e). The decreased current should be resulted from the inert Con A, GOx and alginate molecules which formed the inert coating on electrode and inhibited the electron transfer even through gold nanoparticles had good conductivity. In addition, the negatively charged Con A, GOx and alginate molecules may also block the mass transfer of $Fe(CN)_6^{4-/3-}$ due to the electrostatic repulsion interaction. These phenomena were also confirmed by the electrochemical impedance spectroscopy (EIS) as shown in Fig. 2B. In the Nyquist plot, the diameter of the semi-circle in a higher frequency range is equal to the electron transfer resistance, which represents the electron transfer kinetics of the electroactive

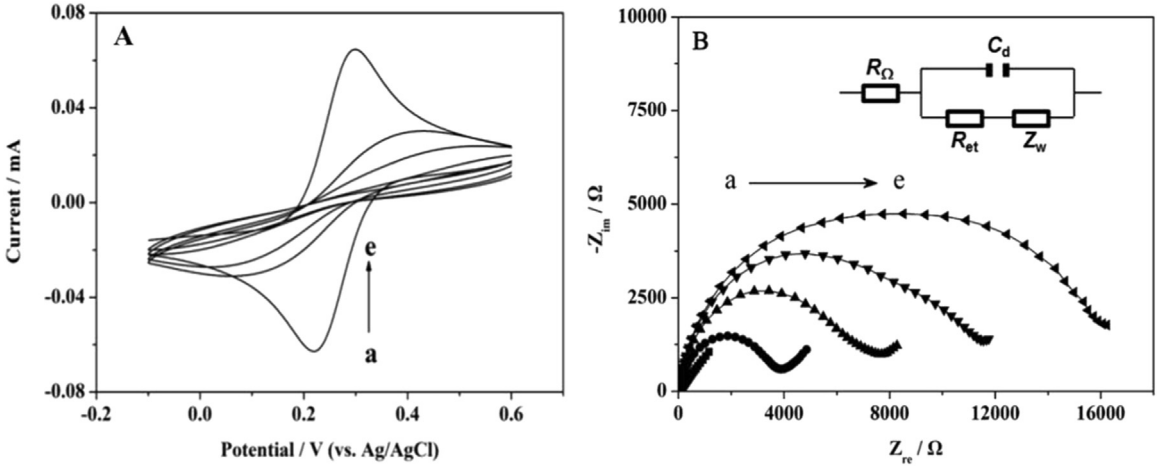

Fig. 2. Cyclic voltammograms (A) and electrochemical impedance spectra (B) of GE (a), WC10/GE (b), Cells/WC10/GE (c), BSA/Cells/WC10/GE (d), GOx@SA-Con A@AuNPs/Cells/WC10/GE (e). These experiments were conducted in 0.1 M KCl solution with 5 mM $[Fe(CN)_6]^{3-/4-}$ electroactive probes. Scan rate, 100 mV s^{-1}. The frequency range was between 0.1 and 10^5 Hz with signal amptitude of 10 mV in panel B. Insert: equivalent circuit of faradic electrochemical impedance (R_Ω: electrolyte resistance, C_d: double layer capacitance, R_{et}: electron transfer resistance, Z_w: Warburg impedance).

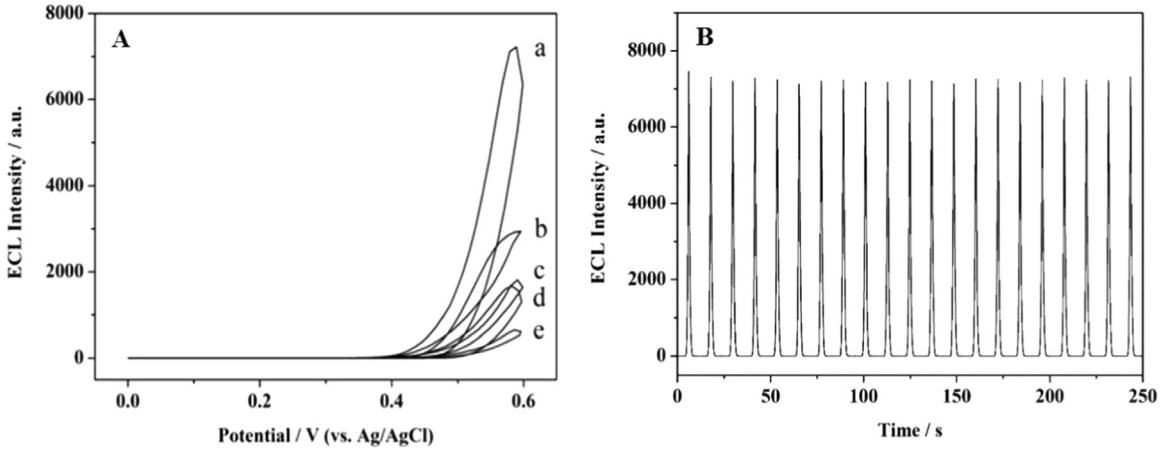

Fig. 3. (A) ECL-potential curves of GOx@SA-Con A@AuNPs/BSA/Cells/WC10/GE (a), GOx@SA-Con A@AuNPs/BSA/Cells/GE (b), GOx@SA/BSA/Cells/WC10/GE (c), GOx@SA-Con A@AuNPs/BSA/WC10/GE (d), Con A@AuNPs/BSA/Cells/WC10/GE (e). (B) ECL-time curve of the GOx@SA-Con A@AuNPs/BSA/Cells/WC10/GE. These experiments were conducted in a 0.1 M PBS (pH 9.0) solution containing 100 μm luminol and 0.1 M glucose. Scan rate, 100 mV s^{-1}. The voltage of PMT was maintained at 600 V.

probes at the electrode interface. It was clear that the diameter of the semicircle after the assembly of WC10 peptides (curve b) and MCF-7 cells (curve c) was larger than that of a bare gold electrode (curve a), indicating an increase of the electron transfer resistance. The electron transfer resistance increased further after the assembly of BSA (curve d) and the signal probes Con A-modified gold nanoparticles and GOx modified alginate (curve e). The phenomena were consistent with those in the CV. The facts elucidate that the gold electrode was step-by-step assembled by WC10 peptides, MCF-7 cells, BSA, and Con A@AuNPs-GOx@SA probes.

3.4. ECL behavior of the biosensor

Fig. 3 presents the ECL responses of the gold electrodes modified with different assembly components in a 0.1 M PBS (pH 9.0) solution containing 100 μm luminol and 0.1 M glucose. The peaks at ca. 0.58 V in ECL curves result from the reaction of luminol. As shown in curve a (Fig. 3A), the GOx@SA-Con A@AuNPs/BSA/Cells /WC10/GE could give the largest ECL signal. When the gold electrode was modified without WC10 peptides, a sharply decrease of ECL response could be seen in curve b. This difference between curve a and b confirms that the strong ECL signal was ascribed to the specific recognition between peptide WC10 and MCF-7 cells, which greatly contributed to the selectivity of the cytosensor. Especially, the ECL signal of curve b was found a bit larger than that of the gold electrode without treatment of MCF-7 cells (curve d). It is because of the nonspecific adsorption of MCF-7 cells onto the electrode without peptides by electrostatic interactions. Moreover, as shown in curve c, after the BSA/Cells/WC10/GE was incubated in GOx@SA probes without pre-incubating in the capture probe Con A@AuNPs, a weak ECL intensity was observed, which could arise from the failure of GOx@SA assembling on the electrode. The result demonstrates that Con A@AuNPs act as an important linker for the immobilization of GOx@SA probes owing to its specific affinity to cell surface glycans, sodium alginate and GOx, allowing the stable and selective absorption of GOx@SA probes on the target cancer cell surface and the following enzymatic signal amplification. Additionally, a weaker ECL intensity was obtained without the signal probe GOx@SA (curve e). The difference between curve a and e certifies that the ECL signal was originated from the GOx mediated electro-oxidation of glucose that produced the H_2O_2 and improved the ECL reaction of luminol. The multiple-site immobilization of GOx and the catalysis of GOx and AuNPs, remarkably amplified the ECL signal, allowing the biosensor to achieve high sensitivity. With GOx@SA as the signal probe, the ECL intensity was observed as ~3 times larger than that with only GOx as the signal probe (Fig. S1 in Supporting Information), demonstrating the remarkable signal amplification effect of the multienzyme decorated polysaccharide. Specially, the ECL emission based on supermolecules assembly approach was very stable. No obvious change was observed upon successive scans (Fig. 3B). These results indicate that ECL could be an effective detection method for this biosensor.

3.5. Optimization of the experimental conditions

The pH of the electrolyte influences significantly on the ECL intensity, which is due to the effect on the activities of cells, efficiency

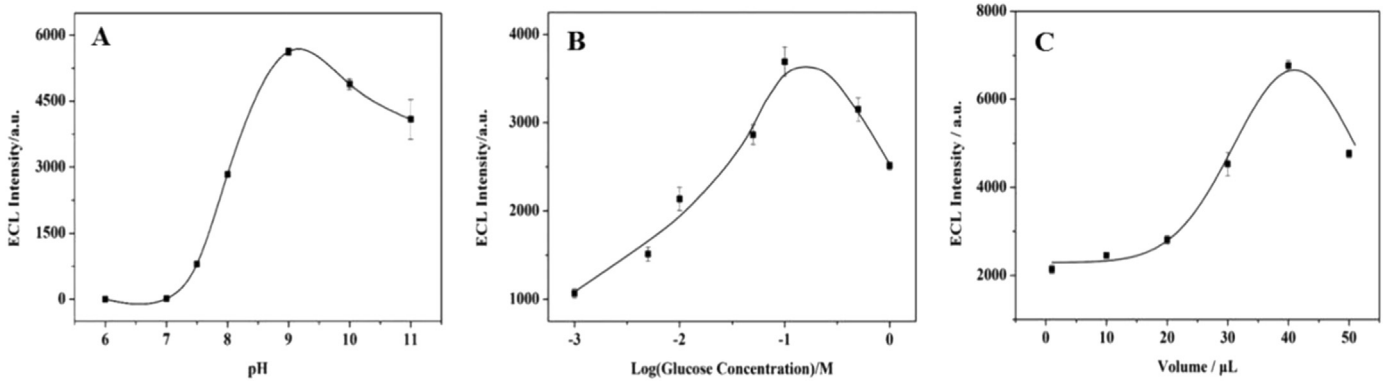

Fig. 4. Dependence of the ECL intensity on (A) different pH of the electrolyte solution, (B) different concentrations of glucose and (C) different volumes of signal probe GOx@SA. The cell concentration, 5×10^5 cells mL^{-1}. The ECL measurements were performed in 0.1 M PBS solution containing 100 μm luminol and 0.1 M glucose. Scan rate, 100 mV s^{-1}. The voltage of PMT was maintained at 600 V.

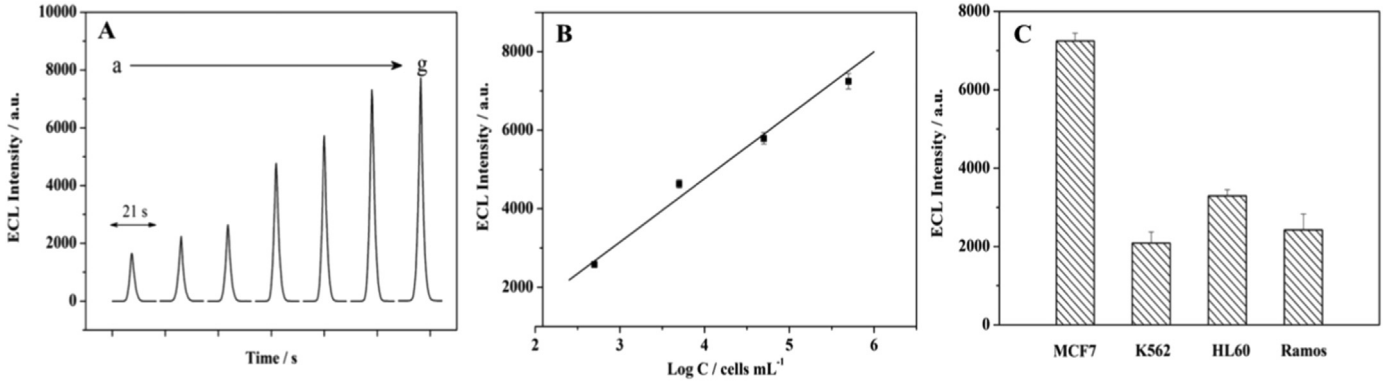

Fig. 5. (A) ECL-time behaviors of GOx@SA-Con A@AuNPs/BSA/Cells/WC10/GE at different concentrations of MCF-7 cells: (a) 0, (b) 5.0×10^{1}, (c) 5.0×10^{2}, (d) 5.0×10^{3}, (e) 5.0×10^{4}, (f) 5.0×10^{5}, and (g) 5.0×10^{6} cells mL^{-1}. These experiments were conducted in a 0.1 M PBS (pH 9.0) solution containing 100 μm luminol and 0.1 M glucose. Scan rate, 100 mV s^{-1}. The voltage of PMT was maintained at 600 V. (B) The linearship between the ECL intensity and the concentration logarithm of MCF-7 cells. (C) The ECL intensity of the electrochemical biosensor with different cell lines at a concentration of 5×10^{5} cells mL^{-1}.

of enzymatic reaction and the aggregation of Con A. Fig. 4A shows the ECL intensity as a function of the pH of the electrolyte solution. It is observed that the signal increased when the pH increased from 6.0 to 9.0 and decreased when the pH increased continually to 11.0. Therefore, a pH of 9.0 was chosen as the experimental pH of the electrolyte in the following experiments.

The responses of the biosensor are dependent importantly on the concentration of glucose and signal probe GOx@SA, which are functioned as co-reactant of the enzymatic reaction. As shown in Fig. 4B, the ECL signal showed an intense increase when the concentration of the glucose increased to 100 mM, and after that a decrease was gotten. Besides, the effect of the signal probe GOx@SA was also investigated as shown in Fig. 4C. When the electrodes modified with Con A@AuNPs were dipped in the solution with different volumes of signal probe GOx@SA, the intensity increased with the volumes increasing to 40 μL and decreased if more volumes were applied. That might be as a result of exorbitant concentration of glucose or signal probe GOx@SA initiating changes of the pH and influenced the ECL intensity. Therefore, the optimal conditions of the biosensor were 100 mM for the concentration of the glucose and 40 μL for the volumes of the signal probe GOx@SA.

3.6. Cytosensing and selectivity of the biosensor

On the basis of the optimal conditions, tumor cells MCF-7 cells were used as the model to determine the sensitivity of the biosensor. As shown in Fig. 5A, the ECL intensity increased with increasing the concentration of the MCF-7 cells. The signal increased linearly with the cells concentration ranging from 5.0×10^{2} to 5.0×10^{5} cells mL^{-1} (Fig. 5B), the detection limit for cells concentration was 150 cells mL^{-1}. Considering that 100 μL of MCF-7 cells were used for incubation, the ECL approach achieved a detection limit of only 15 MCF-7 cells. The as-prepared biosensor with peptides as capture probes and sodium alginate linked glucose oxidase as signal amplification strategy shows excellent sensitivity among the recently reported ECL cytosensors (Han et al., 2011; Chen et al., 2013; Zhou et al., 2014; He et al., 2015; Xin et al., 2016). Moreover, unlike those carbohydrate biosensors merely based on the lectin-carbohydrate interaction, the high affinity between the peptide and cells could improve the binding efficiency between the nanoprobes and thus enhance the sensitivity and the selectivity of the biosensor. Different cell lines such as MCF-7 (human breast adenocarcinoma cell line), K562 (human immortalized myelogenous leukaemia), HL60 (human promyelocytic leukaemia) and Ramos (human burkitt's lymphoma cell line) were chosen as models to evaluate the biosensor selectivity and the ECL intensity is shown in Fig. 5C. Small signal changes were obtained except that for MCF-7, showing the excellent selectivity of the biosensor and that would be a powerful candidate for cancer cell detection.

4. Conclusion

In conclusion, a ECL biosensor for the cancer cell detection was developed by the integration of the peptides modified interface for cell capture, lectin decorated gold nanoparticles acting as the carbohydrate recognition probe as well as glucose oxidase-conjugated sodium alginate as the signal probe. Taking advantage of the high affinity between the peptides and the cancer cells combined with the multivalent recognition of lectin Con A and enzyme catalytic signal amplification process, the as-designed cytosensor showed a low detection limit of 150 cells per mL and a board dynamic range for quantification of cancer cells MCF-7, with excellent sensitivity and stability. Additionally, the ECL biosensor provides a useful tool for evaluating the dynamic profiling of carbohydrate expression on cell membranes. Such a biosensor exhibits great promise in cancer cells detection, clinical diagnosis and treatment of cancer.

Acknowledgement

This work was financially supported by National Natural Science Foundation of China (No. 21621003, No. 21235004, No. 21327806, No. 21622506, No. 21375073), and Tsinghua University Initiative Scientific Research Program.

Appendix A. Supporting information

Supplementary data associated with this article can be found in the online version at doi:10.1016/j.bios.2016.10.040.

References

Ahmed, S., Mathews, A.S., Byeon, N., Lavasanifar, A., Kaur, K., 2010. Anal. Chem. 82, 7533–7541.
Bellapadrona, G., Tesler, A.B., Gruenstein, D., Hossain, L.H., Kikkeri, R., Seeberger, P.H., Vaskevich, A., Rubinstein, I., 2012. Anal. Chem. 84, 232–240.
Cha, C., Shin, S.R., Annabi, N., Dokmeci, M.R., Khademhosseini, A., 2013. ACS Nano 7, 2891–2897.
Chen, Z., Liu, Y., Wang, Y., Zhao, X., Li, J., 2013. Anal. Chem. 85, 4431–4438.
Corti, A., Curnis, F., Arap, W., Pasqualini, R., 2008. Blood 112, 2628–2635.
Dennis, J.W., Nabi, I.R., Demetriou, M., 2009. Cell 139, 1229–1241.
Guo, Y., Li, W., Zheng, M., Huang, Y., 2014. Acta Chim. Sin. 72, 713–719.
Han, E., Ding, L., Jin, S., Ju, H., 2011. Biosens. Bioelectron. 26, 2500–2505.
He, Y., Li, J., Liu, Y., 2015. Anal. Chem. 87, 9777–9785.
Hirabayashi, J., 2008. J. Biochem. 144, 139–147.
Holme, H.K., Davidsen, L., Kristiansen, A., Smidsr, O., 2008. Carbohydr. Polym. 73, 656–664.
Hu, Y., Zuo, P., Ye, B., 2013. Biosens. Bioelectron. 43, 79–83.
Kakehi, K., Oda, Y., Kinoshita, M., 2001. Anal. Biochem. 297, 111–116.
Li, J., Zhu, J., 2013. Analyst 138, 2506–2515.

Linhardt, R.J., Toshihiko, T., 2004. Acc. Chem. Res. 37, 431–438.
Liu, Z., Qi, W., Xu, G., 2015. Chem. Soc. Rev. 44, 3117–3142.
Li, X., Wang, Y., Zhai, J., 2016. Acta Chim. Sin. 74, 597–602.
Lu, X., Wen, Z., Li, J., 2006. Biomaterials 27, 5740–5747.
Marquette, C.A., Blum, L.J., 2009. Anal. Bioanal. Chem. 390, 155–168.
Prang, P., Muller, R., Eljaouhari, A., Heckmann, K., Kunz, W., Webber, T., Faber, C., Vroemen, M., Bogdahn, U., Weidner, N., 2006. Biomaterials 27, 3560–3569.
Rexach, J.E., Clark, P.M., Hsieh-Wilson, L.C., 2008. Nat. Chem. Biol. 4, 97–106.
Richter, M.M., 2004. Chem. Rev. 104, 3003–3036.
Shen, Z., Huang, M., Xiao, C., Zhang, Y., Zeng, X., Wang, P., 2007. Anal. Chem. 79, 2312–2319.
Stangl, S., Varga, J., Freysoldt, B., Trajkovic-Arsic, M., Siveke, J.T., Greten, F.R., Ntziachristos, V., Multhoff, G., 2014. Cancer Res. 74, 6903–6912.
Vedala, H., Chen, Y., Cecioni, S., Imberty, A., Vidal, S., Star, A., 2011. Nano Lett. 11, 170–175.
Veiseh, M., Veiseh, O., Martin, M.C., Asphahani, F., Zhang, M., 2007. Langmuir 2007 (23), 4472–4479.
Wang, M., Sun, C., Wang, L., Ji, X., Bai, Y., Li, T., Li, J., 2003. J. Pharm. Biomed. 33, 1117–1125.
Wang, Y., Lu, J., Tang, L., Chang, H., Li, J., 2009. Anal. Chem. 81, 9710–9715.
Wang, Y., Chen, Z., Liu, Y., Li, J., 2013. Nanoscale 5, 7349–7355.
Wang, Y., Qu, K., Tang, L., Li, Z., Moore, E., Zeng, X., Liu, Y., Li, J., 2014a. Trends Anal. Chem. 58, 54–70.
Wang, Z., Sun, N., He, Y., Liu, Y., Li, J., 2014b. Anal. Chem. 86, 6153–6159.
Wilson, R., Turner, A.P.F., 1992. Biosens. Bioelectron. 7, 165–185.
Xin, X., Yang, Y., Liu, J., Wang, X., Zhou, H., Yu, B., 2016. RSC Adv. 6, 26203–26209.
Xu, S., Liu, Y., Wang, T., Li, J., 2011. Anal. Chem. 83, 3817–3823.
Zhang, J., Spring, H., Schwab, M., 2001. Cancer Lett. 171, 153–164.
Zhang, L., Zhang, Q., Lu, X., Li, J., 2007. Biosens. Bioelectron. 23, 102–106.
Zhang, M., Yuan, R., Chai, Y., Chen, S., Zhong, H., Wang, C., Cheng, Y., 2012. Biosens. Bioelectron. 32, 288–292.
Zhang, Q., Wu, S., Zhang, L., Mao, H., Liu, D., Liu, Y., Zeng, X., Song, X., Li, J., 2014. Acta Chim. Sin. 72, 388–394.
Zhang, Y., Wen, Y., Liu, Y., Li, D., Li, J., 2004. Electrochem. Commun. 6, 1180–1184.
Zhao, Y., Takahashi, M., Gu, J., Miyoshi, E., Matsumoto, A., Kitazume, S., Taniguchi, N., 2008. Cancer Sci. 99, 1304–1310.
Zhou, H., Yang, Y., Li, C., Yu, B., Zhang, S., 2014. Chem. Eur. J. 20, 14736–14743.
Zitzmann, S., Ehemann, V., Schwab, M., 2002. Cancer Res. 62, 5139–5143.